

# Structure and Rearrangement Reactions of Bis(organosilyl)(organostannyl)hydroxylamines: A Joint Theoretical/Experimental Study

Stefan Schmatz,<sup>\*,†</sup> Christina Ebker,<sup>‡</sup> Thomas Labahn,<sup>‡</sup> Hermann Stoll,<sup>§</sup> and Uwe Klingebiel<sup>\*,‡</sup>

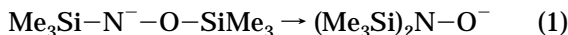
*Institut für Physikalische Chemie and Institut für Anorganische Chemie, Georg-August-Universität Göttingen, Tammannstrasse 4, D-37077 Göttingen, Germany, and Institut für Theoretische Chemie, Universität Stuttgart, Pfaffenwaldring 55, D-70569 Stuttgart, Germany*

Received July 31, 2002

*O*-Lithium-*N,N*-bis(*tert*-butyldimethylsilyl)hydroxylamide reacts with chlorotrimethylstannane to give *N,O*-bis(*tert*-butyldimethylsilyl)-*N*-(trimethylstannyl)hydroxylamine (**1**), the crystal structure of which is presented. The primarily formed *N,N*-bis(*tert*-butyldimethylsilyl)-*O*-(trimethylstannyl)hydroxylamine undergoes a dyotropic rearrangement. This reaction mechanism is corroborated by quantum-chemical calculations (B3LYP), partly employing an effective core potential for tin. The possibility for insertion of a stannyl group has been studied by quantum-chemical calculations. The transition states in the various rearrangement reactions of the bis(organosilyl)stannylhydroxylamine system are discussed in detail.

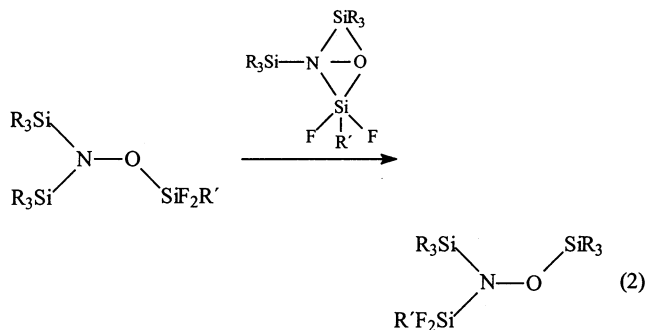
## 1. Introduction

Although lithium silylhydroxylamides have been successfully used in preparative chemistry, e.g. in the preparation of *N,N,O*-tris(silyl)hydroxylamines, since the end of the 1960s,<sup>1</sup> crystal structures of these compounds were described for the first time in 1999/2000.<sup>2,3</sup> The characterized lithium salts form, depending on the bulkiness of the substituents, four-, six-, or eight-membered Li–O–ring systems.<sup>2</sup> When *N,O*-bis(silyl)hydroxylamines are used as the starting materials, this implies a 1,2-anionic silyl group migration from the oxygen to the nitrogen atom.<sup>1,3</sup> The new substituent is primarily bonded to the oxygen atom.



Recently, it could be shown that in reactions with fluorosilanes the formed *O*-(fluorosilyl)-*N,N*-bis(organosilyl)hydroxylamines undergo an irreversible rearrangement, yielding the isomeric *N*-(fluorosilyl)-*N,O*-bis(organosilyl)hydroxylamines (see Scheme 2).<sup>4</sup>

Mitzel and Losehand pointed out that *O*-silyl-*N*-alkylhydroxylamines are able to form intramolecular donor–acceptor bonds between silicon and nitrogen centers separated by one oxygen atom only.<sup>5</sup> These



strong  $\beta$ -donor interactions could help to explain the easy silyl group migrations in tris(silyl)hydroxylamines. Fluorosilyl groups prefer to be bonded to the—compared with the oxygen atom—softer Lewis base, the nitrogen atom.<sup>4</sup>

It was shown by density functional calculations<sup>4</sup> and synthetic methods<sup>1,6,7</sup> that the isomerizations proceed via dyotropic transition states. These first-order saddle points on the potential energy surface can be described as bicyclic structures with the N–O unit bridged by two silyl groups. Recently, several model compounds were investigated, and trends for the migration of differently substituted silyl groups via dyotropic transition states were reported.<sup>8</sup> It is not self-evident that similar dyotropic rearrangement reactions may take place in hydroxylamines containing germyl or stannyl groups, because these groups are much bulkier than silyl groups so that the acute angles in the corresponding dyotropic transition states are even smaller. It may be anticipated

<sup>†</sup> Institut für Physikalische Chemie, Georg-August-Universität Göttingen.

<sup>‡</sup> Institut für Anorganische Chemie, Georg-August-Universität Göttingen.

<sup>§</sup> Universität Stuttgart.

(1) Boudjouk, P.; West, R. *Intra-Sci. Chem. Rep.* **1973**, 7, 65.

(2) Diedrich, F.; Klingebiel, U.; Dall'Antonia, F.; Lehmann, C.; Noltemeyer, M.; Schneider, T. R. *Organometallics* **2000**, 19, 5376.

(3) Diedrich, F.; Klingebiel, U.; Schäfer, M. *J. Organomet. Chem.* **1999**, 588, 242.

(4) Wolfram, R.; Müller, T.; Klingebiel, U. *Organometallics* **1998**, 17, 3222.

(5) Mitzel, N. W.; Losehand, U. *J. Am. Chem. Soc.* **1998**, 120, 7320.

(6) West, R.; Boudjouk, P. *J. Am. Chem. Soc.* **1973**, 95, 3983.

(7) Nowakowski, P.; West, R. *J. Am. Chem. Soc.* **1976**, 98, 5616.

(8) Schmatz, S.; Diedrich, F.; Ebker, C.; Klingebiel, U. *Eur. J. Inorg. Chem.* **2002**, 4, 876.

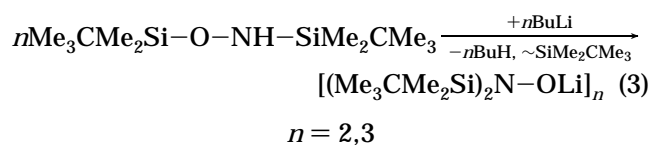
that these transition states are higher in energy than those reported in ref 8, so that a thermal dyotropic rearrangement is less favorable for stannylhydroxylamines. In this paper we present the synthesis and the X-ray structure of the first *N,O*-bis(silyl)-*N*-stannylhydroxylamine. It is shown by quantum-chemical calculations that the reaction pathway yielding this species indeed includes passing through a dyotropic transition state.

The insertion of silyl groups into the N–O bond, yielding disiloxane, was studied both experimentally<sup>1</sup> and theoretically,<sup>8</sup> emphasizing the reaction mechanisms and the pertinent transition states. Preferences for insertion were discussed in detail. The question arises as to whether the insertion of a stannyl group into the N–O bond is also possible. While this insertion could not yet be observed experimentally, quantum-chemical calculations can give more insight into this rearrangement process.

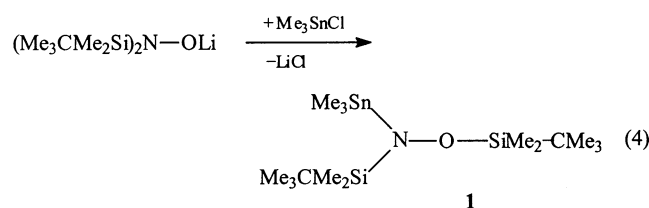
This paper is organized as follows: Section 2 reports the synthesis of the *N,O*-bis(silyl)-*N*-stannylhydroxylamine and its crystallographic characterization. Section 3 contains the quantum-chemical study of the dyotropic rearrangement reaction of this novel class of compounds as well as the insertion of stannyl or silyl groups into the N–O bond.

## 2. Experimental Results and Discussion

**2.1. Synthesis of *N,O*-Bis(*tert*-butyldimethylsilyl)-*N*-(trimethylstannyl)hydroxylamine.** For the preparation of the stannylhydroxylamine we used *N,O*-bis(*tert*-butyldimethylsilyl)hydroxylamine, which with BuLi forms a dimer via a (Li–O)<sub>2</sub> four-membered ring in THF and a trimer via a (Li–O)<sub>3</sub> six-membered ring in hexane. In both solvents (Me<sub>3</sub>CSiMe<sub>2</sub>)<sub>2</sub>N–O<sup>–</sup> anions are formed. This means that a silyl group migration from oxygen to nitrogen has occurred.<sup>2</sup>



For that reason a new silyl- or stannyl- group is attached to the oxygen atom. However, in the reaction of chlorotrimethylstannane and this lithium salt we were only able to isolate the *N,O*-bis(*tert*-butyldimethylsilyl)-*N*-(trimethylstannyl)hydroxylamine.



Under the experimental conditions the primarily formed *O*-stannylhydroxylamine could not be detected. The formation of **1** can be explained by the HSAB concept. The soft Lewis base tin tries to bond to the soft Lewis base nitrogen. This result implies a 1,2-stannyl group migration from oxygen to nitrogen and a silyl group migration from the nitrogen to the oxygen atom via a dyotropic transition state.

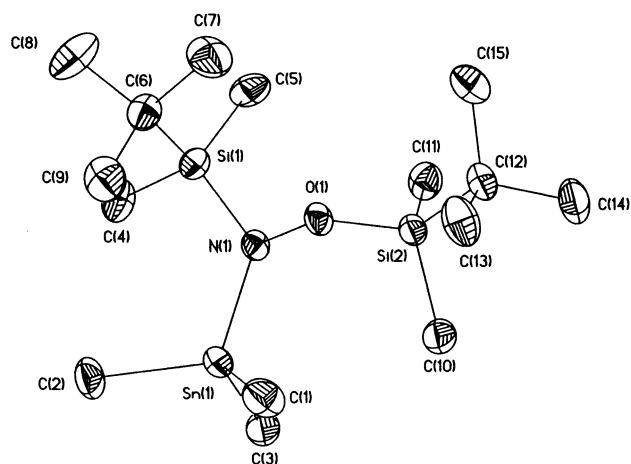
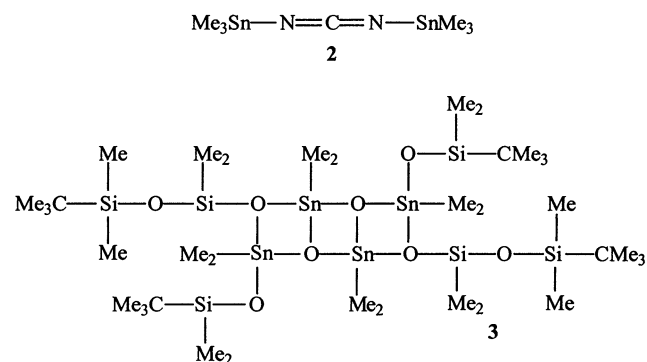


**Figure 1.** Crystal structure of *N,O*-bis(*tert*-butyldimethylsilyl)-*N*-(trimethylstannyl)hydroxylamine (compound **1**). Selected bond lengths (Å) and angles (deg): Sn(1)–N(1) = 2.088(3), N(1)–Si(1) = 1.749(3), N(1)–O(1) = 1.497(3), O(1)–Si(2) = 1.666(2), Sn(1)–C(3) = 2.143(4), Si(1)–C(4) = 1.882(4), Si(1)–C(6) = 1.902(4), Si(2)–C(10) = 1.866(4), Si(2)–C(12) = 1.892(4); O(1)–N(1)–Si(1) = 105.36(17), Si(1)–N(1)–Sn(1) = 126.57(14), O(1)–N(1)–Sn(1) = 108.59(16), N(1)–O(1)–Si(2) = 115.70(18), N(1)–Sn(1)–C(1) = 105.76(12), N(1)–Si(1)–C(5) = 110.13(15), N(1)–Si(1)–C(4) = 105.23(17), N(1)–Si(1)–C(6) = 114.83(14), O(1)–Si(2)–C(10) = 111.78(14), O(1)–Si(2)–C(12) = 101.83(14).

Attempts to carry out insertion reactions of a dimethylstannyl group or a dimethylsilyl group into the N–O bond under the right reaction conditions, which was successfully done in tris(silyl)hydroxylamine chemistry,<sup>1,8</sup> failed until now. In a not transparent, complex reaction we were able to isolate bis(trimethylstannyl)-carbodiimide (**2**), which was described in 1971,<sup>9</sup> and the dimeric 1,7,9-trisilyl-3,5-distannyl-2,4,6,8-tetraoxane **3**.



The formation of **3** may indicate that a dimethylsilyl group with migration of a *tert*-butyl group to the nitrogen as well as a dimethylstannyl group with migration of a methyl group are able to insert into the N–O bond.

**2.2. Crystal Structure of *N,O*-Bis(*tert*-butyldimethylsilyl)-*N*-(trimethylstannyl)hydroxylamine.** Crystals of **1** were obtained from a solution in *n*-hexane at 0 °C. The crystal structure of **1** is depicted in Figure 1. The crystals belong to the orthorhombic space group *Pbca* with eight molecules in the unit cell (see Table 1). There are no transannular Si(2)⋯N(1) or Sn(1)⋯O(1) contacts, as found in methylhydroxylamines.<sup>5</sup> The ni-

**Table 1. Crystallographic Data for Compound 1**

empirical formula	C <sub>15</sub> H <sub>39</sub> NOSi <sub>2</sub> Sn
fw	424.34
color of cryst	colorless
temp (K)	133(2)
cryst size (mm)	0.5 × 0.5 × 0.4
cryst syst	orthorhombic
space group	<i>Pbca</i>
<i>a</i> (Å)	10.939(2)
<i>b</i> (Å)	13.122(3)
<i>c</i> (Å)	30.561(6)
α (deg)	90
β (deg)	90
γ (deg)	90
cell vol (Å <sup>3</sup> )	4386.9(15)
<i>Z</i>	8
ρ <sub>c</sub> (mg mm <sup>-3</sup> )	1.285
μ (mm <sup>-1</sup> )	1.273
<i>F</i> (000)	1776
2θ range (deg)	1.33–25.06
no. of data measd	46 408
no. of unique data	3805 ( <i>R</i> <sub>int</sub> = 0.1123)
<i>R</i> <sub>1</sub> , <i>wR</i> <sub>2</sub> <sup>a</sup> ( <i>I</i> > 2σ( <i>I</i> ))	0.0356, 0.1123
<i>R</i> <sub>1</sub> , <i>wR</i> <sub>2</sub> (all data)	0.0361, 0.1132
goodness of fit, <i>S</i> <sup>c</sup>	1.079
no. of refined params	181
largest diff peak/hole (e Å <sup>-3</sup> )	0.704/−0.788

$$^a R_1 = \sum |F_o| - |F_c| / \sum |F_o|, \quad ^b wR_2 = \{[\sum w(F_o^2 - F_c^2)^2] / [\sum w(F_o^2)^2]\}^{1/2},$$

$$^c S = \{[\sum w(F_o^2 - F_c^2)^2] / [\sum (n - p)]\}^{1/2}.$$

trogen atom exhibits an almost pyramidal coordination sphere (sum of angles N(1) 340.5°) with one valence angle between the silyl and the stannyl groups substantially wider (126.5°) than the other two angles. The distance to the plane of the neighboring atoms O(1), Si(1), and Sn(1) amounts to 45.26 pm. This is in contrast to silylhydrazines and silylamines, where normally a planar coordination of the nitrogen atom is found. In silylhydroxylamines the oxygen atom leads to a significant change of the polarity at the nitrogen atom and therefore to pyramidal instead of planar surroundings for the nitrogen atom.<sup>10,11</sup>

### 3. Quantum-Chemical Study of the Rearrangement Reactions of Bis(silyl)stannylhydroxylamines

**3.1. Methodology.** To elucidate the rearrangement processes that are possible in the chemistry of this novel class of compounds, quantum-chemical (density functional, DFT) calculations have been carried out. The calculations were performed for isolated molecules in the gas phase, the results of which may be compared with experimental data obtained in aprotic or nonpolar solvents (*n*-hexane).

To reduce the computational expense, the calculations were carried out for *N*,*O*-bis(trimethylsilyl)-*N*-(trimethylstannyl)hydroxylamine (**A**) instead of *N*,*O*-bis(*tert*-butyldimethylsilyl)-*N*-(trimethylstannyl)hydroxylamine. The structures of the stationary points **A**, **B**, **PA**, **PB1**, **PB2**, **TSd**, **TSA**, **TSB1**, and **TSB2** (see Figure 2) on the potential energy hypersurface (PES) were fully optimized using Becke's three-parameter hybrid method with Becke's exchange functional<sup>12</sup> and the Lee, Yang, and Parr correlation functional<sup>13</sup> (B3LYP). To confirm

(10) Wolfgramm, R.; Klingebiel, U.; Noltemeyer, M. *Z. Anorg. Allg. Chem.* **1998**, *624*, 865.

(11) Mitzel, N.; Angermaier, K.; Schmidbaur, H. *Organometallics* **1994**, *13*, 1762.

(12) Becke, A. D. *J. Chem. Phys.* **1993**, *98*, 5648.

that true minima on the PES were found, the Hessian matrices at the stationary points were calculated. The energies were further corrected for zero-point vibrational effects, which, however, are usually only of minor importance in isomerization reactions. The TS routine of GAUSSIAN98<sup>14</sup> and the intrinsic reaction coordinate (IRC) method<sup>15</sup> were employed for the calculation of the transition state (first-order saddle point) geometries.

The structures were first optimized employing the very small 3-21G basis set (212 contracted Gaussian-type orbitals (cGTOs) for C<sub>9</sub>H<sub>27</sub>NOSi<sub>2</sub>Sn) that does not contain any d functions at the first-row atoms. Since tin is not supported by the standard 6-31G(d) basis which was used in most of our previous theoretical studies on silylhydroxylamines<sup>8</sup> and silylhydrazines,<sup>16–20</sup> we performed our second series of calculations with a DZVP (DFT orbital) basis set<sup>21</sup> which for first- and second-row atoms is briefly described as H [2s], Li–Ne [3s,2p,1d], Na–Ar [4s,3p,1d] and is thus comparable to the 6-31G(d) set (H [2s], Li–Ne [3s,2p,1d], Na–Ar [4s,3p,1d]). For Sn<sup>22</sup> the DZVP basis is described as [6s,5p,3d]. It comprises 280 cGTOs for C<sub>9</sub>H<sub>27</sub>NOSi<sub>2</sub>Sn.

Relativistic effects are of importance in tin and should not be neglected. For instance, the bond lengths are subject to a reduction if the relativistic motion of the electrons is taken into account. For systems of the size of the bis(silyl)stannylhydroxylamines, four-component all-electron relativistic calculations are out of the question presently, and even quasi-relativistic computations are extremely costly. A way to circumvent these problems is the use of relativistic pseudopotentials (also termed effective core potentials (ECP)), which have the additional advantage that not all electrons of the heavy element have to be taken into account explicitly.

We thus made use of a pseudopotential for tin. A [3s,3p,1d] basis set is used for the valence electrons and the scalar-relativistic Stuttgart SN-46-MWB pseudopotential (PP)<sup>23</sup> for the description of the core. The

(13) Lee, C.; Yang, W.; Parr, R. G. *Phys. Rev. B* **1988**, *37*, 785.

(14) Frisch, M. J.; Trucks, G. W.; Schlegel, H. B.; Scuseria, G. E.; Robb, M. A.; Cheeseman, J. R.; Zakrzewski, V. G.; Montgomery, J. A., Jr.; Stratmann, R. E.; Burant, J. C.; Dapprich, S.; Millam, J. M.; Daniels, A. D.; Kudin, K. N.; Strain, M. C.; Farkas, O.; Tomasi, J.; Barone, V.; Cossi, M.; Cammi, R.; Mennucci, B.; Pomelli, C.; Adamo, C.; Clifford, S.; Ochterski, J.; Petersson, G. A.; Ayala, P. Y.; Cui, Q.; Morokuma, K.; Malick, D. K.; Rabuck, A. D.; Raghavachari, K.; Foresman, J. B.; Cioslowski, J.; Ortiz, J. V.; Stefanov, B. B.; Liu, G.; Liashenko, A.; Piskorz, P.; Komaromi, I.; Gomperts, R.; Martin, R. L.; Fox, D. J.; Keith, T.; Al-Laham, M. A.; Peng, C. Y.; Nanayakkara, A.; Gonzalez, C.; Challacombe, M.; Gill, P. M. W.; Johnson, B. G.; Chen, W.; Wong, M. W.; Andres, J. L.; Head-Gordon, M.; Replogle, E. S.; Pople, J. A. *Gaussian 98*, revision A.7; Gaussian, Inc.: Pittsburgh, PA, 1998.

(15) Gonzalez, C.; Schlegel, H. B. *J. Chem. Phys.* **1989**, *90*, 2154; *J. Phys. Chem.* **1990**, *94*, 5523.

(16) Gellermann, E.; Klingebiel, U.; Pape, T.; Dall'Antonia, F.; Schneider, T. R.; Schmartz, S. *Z. Anorg. Allg. Chem.* **2001**, *627*, 2581.

(17) Gellermann, E.; Klingebiel, U.; Noltemeyer, M.; Schmartz, S. *J. Am. Chem. Soc.* **2001**, *123*, 378.

(18) Schmartz, S. *J. Phys. Chem. A* **2001**, *105*, 3875.

(19) Klingebiel, U.; Schmartz, S.; Gellermann, E.; Drost, C.; Noltemeyer, M. *Monatsh. Chem.* **2001**, *132*, 1105.

(20) Schmartz, S. *Organometallics* **2002**, *21*, 864.

(21) Godbout, N.; Salahub, D. R.; Andzelm, J.; Wimmer, E. *Can. J. Chem.* **1992**, *70*, 560.

(22) Salahub, D. R. Private communication. See also: <http://www.pnl.gov> (Pacific Northwest Laboratory).

(23) Bergner, A.; Dolg, M.; Kuechle, W.; Stoll, H.; Preuss, H. *Mol. Phys.* **1993**, *80*, 1431. See also the PP database on <http://www.theochem.uni-stuttgart.de/pseudopotentials>.



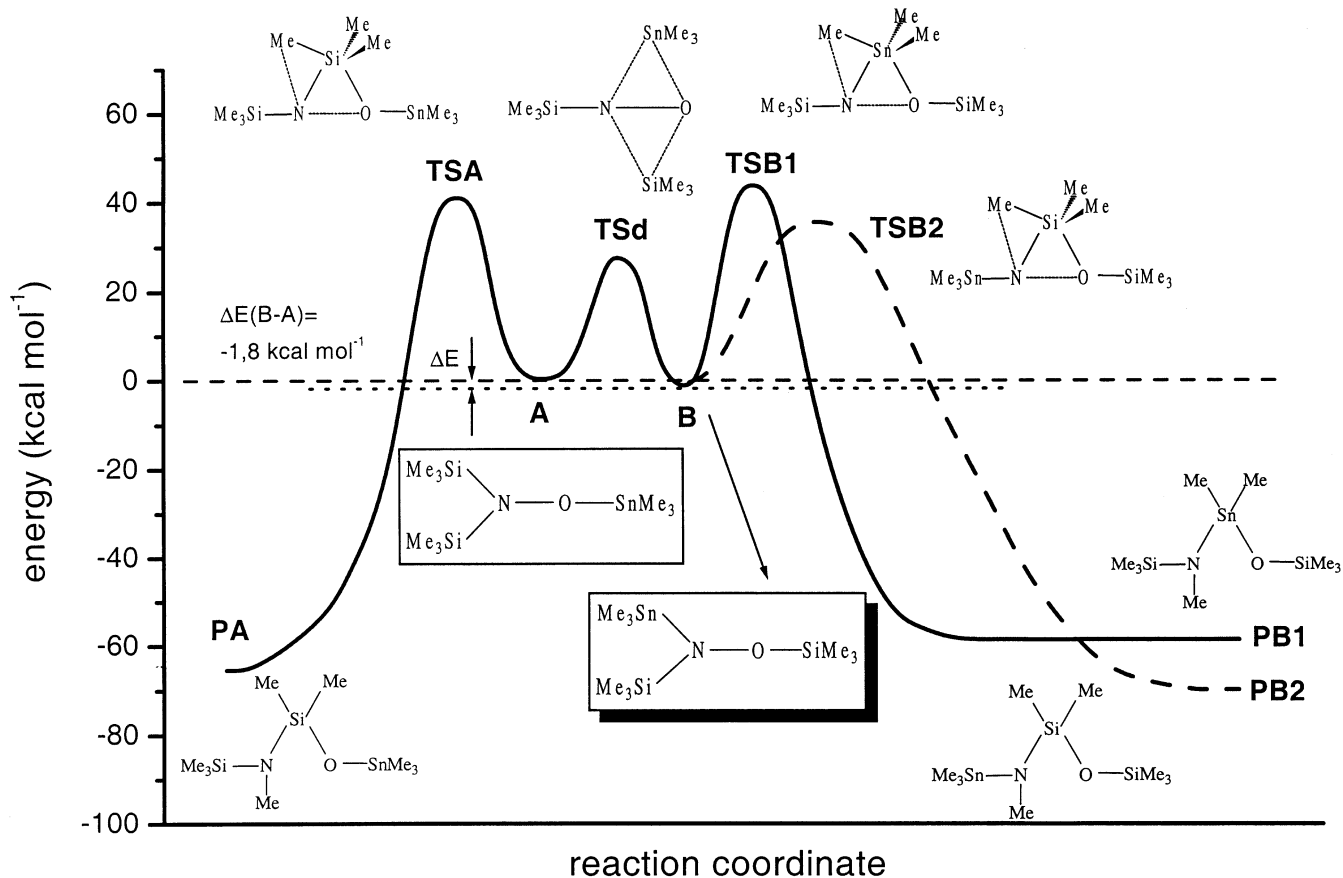


**Figure 2.** Potential energy diagram (schematic) for the isomers of the *N,O*-bis(trimethylsilyl)-*N*-(trimethylstannyl)-hydroxylamine system. The abscissa does not correspond to any well-defined reaction coordinate. Energetic differences are taken from B3LYP/6-31G(d)+PP calculations (see the text).

6-31G(d) basis was employed for C, O, N, Si, and H. In all, 261 cGTOs were included in this basis (denoted 6-31G(d)+PP).

At the B3LYP/6-31G(d)+PP optimized geometries of the nine structures single-point B3LYP calculations were carried out using the *s*, *p*, and *d* functions of the cc-pVTZ<sup>24</sup> set for C, O, N, and Si and its *s* and *p* functions for H. For Sn the recent correlation-consistent pseudopotential basis set of cc-pVTZ quality was employed (without *f* functions) that has been optimized by Martin and Sundermann<sup>25</sup> for use with the Stuttgart–Dresden–Bonn (SDB) relativistic pseudopotentials. This basis is denoted VTZ+PP and comprises 572 cGTOs.

Finally, single-point second-order perturbation calculations according to Møller and Plesset (MP2) were carried out at the B3LYP/6-31G(d)+PP geometries of the stationary points for comparison with the DFT results. The 6-31G(d)+PP basis was used in the MP2 calculations.

**3.2. Dyotropic Rearrangement of Bis(silyl)stannylhydroxylamines.** The equilibrium structures of the two hydroxylamines and the saddle point corresponding to the dyotropic transition state are given in Table 2. The geometries of the *N,N*-bis(silyl)-*O*-stannylhydroxylamine (**A**) and the *N,O*-bis(silyl)-*N*-stannylhydroxyl-

amine (**B**) are comparable with those reported for the tris(silyl)hydroxylamines.<sup>8</sup> The Sn–O and Sn–N bond distances are calculated to be 204.4 and 211.5 pm, respectively. Without employment of the pseudopotential (i.e. DZVP basis set), the values are larger by 2.2 and 1.4 pm, respectively. The effective core potential accounts for relativistic effects and yields a reduction of the bond length. The Sn–N bond in the crystal was determined to be 208.8 pm. Thus, the B3LYP/6-31G(d)+PP result overestimates the experimental value by 1.3%. The deviations of the theoretical bond distances (Table 2) and the experimental results (Figure 1) amount to –0.6 pm (N–O), 2.5 pm (N–Si), and 3.4 pm (O–Si). The harmonic vibrational wavenumber of the Sn–N stretching mode in **B** is calculated to be 461 cm<sup>–1</sup> (B3LYP/6-31G(d)+PP) and 468 cm<sup>–1</sup> (B3LYP/DZVP), respectively.

Species **A** exhibits *C<sub>s</sub>* symmetry with trans conformation of the substituents at the oxygen and nitrogen atoms. The lone electron pair at nitrogen may undergo a  $\beta$ -donor interaction<sup>5</sup> with unoccupied orbitals at the tin atom. In **B**, the respective interaction takes place between the lone electron pair at nitrogen and the unoccupied orbitals at the silicon atom attached to the oxygen atom.

It could be shown that in tris(silyl)hydroxylamines dyotropic rearrangements take place.<sup>4,8</sup> Those silyl groups that are harder Lewis bases tend to the oxygen atom, whereas the weaker Lewis acidic silyl substituents prefer the softer base nitrogen. Theoretical inves-

(24) Dunning, T. H., Jr. *J. Chem. Phys.* **1989**, *90*, 1007. Woon, D. E.; Dunning, T. H. *J. Chem. Phys.* **1993**, *98*, 1358.

(25) Martin, J. M. L.; Sundermann, A. *J. Chem. Phys.* **2001**, *114*, 3408.

**Table 2. B3LYP/DZP (left) and B3LYP/6-31G(d)+PP (right) Geometries of the Nine Stationary Points<sup>a</sup>**

	<b>A</b>	<b>TSd</b>	<b>B</b>	<b>TSA</b>	<b>PA</b>	<b>TSB1</b>	<b>PB1</b>	<b>TSB2</b>	<b>PB2</b>
$r(\text{N}-\text{O})$	148.7/148.6	156.0/156.4	149.2/149.1	205.9/206.2	280.7/281.6	231.9/230.2	332.1/328.4	205.2/205.5	268.8/281.0
$r(\text{N}-\text{Si}')$	176.9/177.1	181.6/181.3	177.4/177.4	177.4/177.5	176.0/176.2	177.0/177.2	175.3/175.6	170.6/170.7	172.5/173.6
$r(\text{N}-\text{Si}'')$	176.9/177.1	186.2/186.4		170.5/170.8	175.8/176.0				
$r(\text{O}-\text{Sn})$	206.6/204.4	242.7/238.1		204.5/202.1	202.0/199.8	217.7/216.3	201.7/199.4		
$r(\text{O}-\text{Si}')$								191.5/190.6	166.9/166.6
$r(\text{O}-\text{Si}'')$		201.4/198.9	170.0/169.9	184.4/183.8	165.0/165.3	166.3/166.5	165.5/165.7	167.8/167.9	166.9/166.0
$r(\text{N}-\text{Sn})$		222.0/222.3	213.0/211.5			206.7/204.5	207.0/205.3	212.4/211.3	209.4/208.0
$r(\text{C}^*-\text{Sn})$	217.4/216.2		218.1/216.5			235.1/236.0	303.7/302.2		
$r(\text{C}^*-\text{N})$				248.4/248.7	148.0/147.5	270.4/268.2	147.8/147.3	246.4/246.8	147.3/147.4
$r(\text{C}^*-\text{Si})$	188.9/189.3		189.0/189.0	211.3/211.7	279.6/279.8			208.2/208.8	275.0/273.5
$\alpha(\text{Si}'-\text{N}-\text{Si}'')$	131.8/131.5	122.6/122.2		138.3/137.9	125.9/125.8				
$\alpha(\text{Si}'-\text{N}-\text{O})$	106.3/105.7	116.0/115.6	108.4/108.4					60.4/60.0	
$\alpha(\text{Si}''-\text{N}-\text{O})$	106.3/105.7	71.5/70.3		57.8/57.4	33.3/33.2				
$\alpha(\text{N}-\text{O}-\text{Sn})$	115.9/116.2	63.4/64.8				54.7/54.4	36.2/36.4		
$\alpha(\text{Sn}-\text{N}-\text{O})$		77.7/75.7	107.1/107.1			59.0/59.3	35.1/35.2		
$\alpha(\text{N}-\text{O}-\text{Si}'')$		61.3/61.9	116.4/116.5	51.5/51.6	35.8/35.7				
$\alpha(\text{Si}'-\text{N}-\text{Sn})$		118.2/119.4	120.0/120.8			133.7/134.2	124.2/124.2	131.0/88.8	122.1/125.9
$\alpha(\text{O}-\text{Sn}-\text{N})$		38.9/39.5				66.3/66.3	108.7/108.4		
$\alpha(\text{O}-\text{Si}''-\text{N})$		47.3/47.7		71.0/71.0	110.8/111.1				
$\alpha(\text{N}-\text{Si}'-\text{O})$								68.8/69.1	104.7/111.4
$\alpha(\text{Si}'-\text{O}-\text{Si}'')$								142.7/142.2	144.4/152.5
$\alpha(\text{Si}''-\text{O}-\text{Sn})$				135.4/135.7	139.5/139.9	142.1/142.4	142.0/142.0		
$\theta(\text{Si}'-\text{N}-\text{O}-\text{Sn})$	-108.1/-108.6	-115.6/-116.1		-101.2/-101.0	-89.5/-90.1	128.7/129.3	136.3/137.0		
$\theta(\text{Si}''-\text{N}-\text{O}-\text{Sn})$	108.1/108.6	126.5/126.8							
$\theta(\text{Si}'-\text{N}-\text{O}-\text{Si}'')$		117.9/117.1	118.0/117.1	133.6/133.0	141.0/139.2	-99.3/-98.3	-93.1/-92.2	132.6/132.4	
$\theta(\text{Sn}-\text{N}-\text{O}-\text{Si}'')$		-126.5/-126.8	-111.2/-111.0			132.0/132.4		-100.6/-99.3	-71.8/74.1
$\theta(\text{O}-\text{Sn}-\text{N}-\text{Si}'')$		-60.6/-58.3							
$\theta(\text{Si}'-\text{N}-\text{Sn}-\text{O})$		113.1/111.6				-92.1/-92.2	-55.1/-54.2		
$\theta(\text{N}-\text{Sn}-\text{O}-\text{Si}'')$						-110.8/-109.2	-83.0/-82.9		
$\theta(\text{Sn}-\text{N}-\text{Si}'-\text{O})$								-90.9/-87.4	-6.5/125.9
$\theta(\text{N}-\text{Si}'-\text{O}-\text{Si}'')$								-100.4/-98.8	-166.2/-43.8

<sup>a</sup> Bond lengths  $r$  are given in pm and bond angles  $\alpha$  in deg. The asterisk denotes the carbon atom of the transferred methyl group.

Table 3. Energetics (in kcal mol<sup>-1</sup>) of the Nine Stationary Points<sup>a</sup>

	A	TSd	B	TSA	PA	TSB1	PB1	TSB2	PB2
$\Delta E$ (B3LYP/3-21G)	0.0	23.5	-0.88	43.7	-62.0	39.6	-58.2	37.7	-65.2
$\Delta E$ (B3LYP/DZVP)	0.0	28.0	-2.74	42.4	-64.6	42.6	-57.4	36.4	-70.6
$\Delta E$ (B3LYP/6-31G(d)+PP)	0.0	28.3	-1.76	41.6	-65.4	44.7	-58.5	36.8	-69.7
$\Delta E$ (B3LYP/VTZ+PP) <sup>b</sup>	0.0	29.1	-2.63	41.8	-63.0	43.7	-57.1	36.5	-68.7
$\Delta E$ (MP2/6-31G(d)+PP) <sup>b</sup>	0.0	22.4	-1.00	54.4	-69.3	65.6	-62.6	51.2	-72.1
$\Delta(E + E_{zp})$ (B3LYP/6-31G(d)+PP)	0.0	28.2	-1.64	40.2	-63.6	42.8	-57.0	35.2	-67.9
$\Delta^\circ H_{\text{R}}(298)$ (B3LYP/6-31G(d)+PP)	0.0		-1.76		-63.7		-57.0		-68.1

<sup>a</sup> Different methods and basis sets; see text for details. <sup>b</sup> At the B3LYP/6-31G(d)+PP geometries of the stationary points.

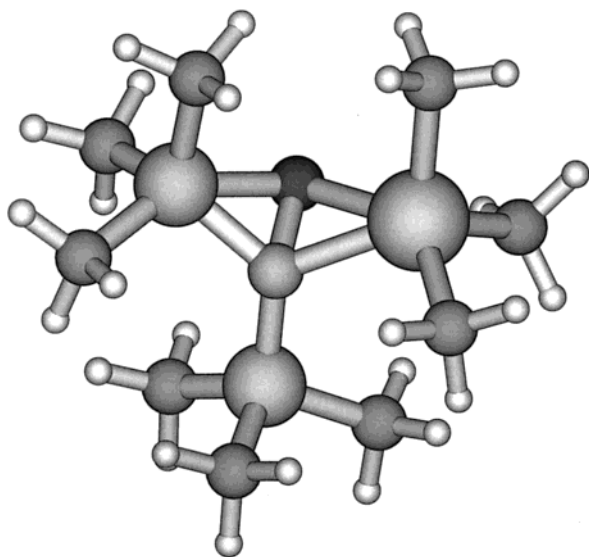


**Figure 3.** B3LYP/6-31G(d)+PP structure of the dyotropic transition state (TSd). See the text and Figure 2 for details.

tigations have shown that this isomerization proceeds via a dyotropic transition state which is a bicyclic structure with the N–O unit bridged by two silyl groups. The angles of the two acute triangles present in this structure at the migrating groups are relatively small (about 45°<sup>8</sup>). The quantum-chemical finding that such a structure could in fact be calculated was quite surprising and not a priori expected, even if the dyotropic mechanism was postulated several years ago.<sup>26</sup>

It was not clear whether such a mechanism could also be observed for higher homologues of silicon, viz. germanium and tin. The density functional (B3LYP/6-31G(d)+PP) calculations support the existence of a dyotropic transition state for reaction **A** → **B** with an acute angle of 39.5° at the migrating tin atom (see Figure 3). The acute angle at the migrating silicon atom is calculated to be 47.7°, in good agreement with the results from ref 8. The N–O bond distance is slightly larger compared to the tris(silyl)hydroxylamines. The DZVP Sn–O distance is larger by 4.6 pm compared to the 6-31G(d)+PP result (238.1 pm), whereas the Sn–N distance is smaller by 0.3 pm.

The energetics of the isomerization process are presented in Table 3. **B** is more stable than **A** by 1.8 kcal mol<sup>-1</sup>. This result is supported by calculations with various methods and basis sets (see Table 3) and is mainly due to the presence of a strong silicon–oxygen bond in **B**. B3LYP with the larger VTZ+PP basis increases  $\Delta E(\mathbf{A}-\mathbf{B})$  to 2.6 kcal mol<sup>-1</sup>, whereas MP2 with

a 6-31G(d)+PP basis set decreases this value to 1.0 kcal mol<sup>-1</sup>. Zero-point energy effects only slightly influence this energetic difference (decrease by 0.1 kcal mol<sup>-1</sup>), due to the very similar structures of the two isomers. The inclusion of thermal effects (298 K) raises the difference of the isomers, again yielding -1.8 kcal mol<sup>-1</sup> for the reaction enthalpy.

The classical barrier to isomerization is relatively small (28.3 kcal mol<sup>-1</sup>), so that the reaction can indeed proceed via this mechanism under the experimental conditions. The barrier height is slightly smaller than for simultaneous migration of two silyl groups.<sup>8</sup>

The reactive normal mode of the first-order saddle point structure is displayed graphically in Figure 4. It can clearly be seen that the tin atom is almost at rest, whereas the overall characteristic motion can be described as a rotation of the NO moiety (and, of course, the motion of the methyl groups at the migrating centers). The reduced mass for the rotation of a NO unit about its center of mass amounts to 7.5 amu, which is quite close to  $\mu_{\text{TSd}} = 9.3$  amu for the reactive mode of the dyotropic transition state. Due to the heavy tin atom the harmonic vibrational frequency of this normal mode (231 cm<sup>-1</sup>) is slightly smaller than found for the tris(silyl)hydroxylamines.<sup>8</sup>

**3.3. Insertion of Silyl and Stannyl Groups into the N–O Bond.** The insertion of silyl groups into the N–O bond was discussed in detail.<sup>1,8</sup> The products were identified as disiloxanes. The reaction mechanisms could be corroborated by DFT calculations. The transition states exhibit an almost planar five-center structure which can also be regarded as a bicyclic structure. In the present experimental study of bis(silyl)stannylhydroxylamines such an insertion was not observed; neither disiloxanes nor stannylsiloxanes were formed. This should not imply that such an insertion is impossible in principle.

To find out which product is more stable, the disiloxanes **PA** (starting from reactant **A** without dyotropic rearrangement yielding **B**) and **PB2** or the stannylsiloxane **PB1**, density functional (B3LYP) calculations have been carried out for the three structures.

The equilibrium geometries of the three possible products are given in Table 2. While the differences of the geometries obtained with the DZVP and 6-31G(d)+PP basis sets are vanishingly small for **PA** and **PB1** (with the exception of the bond distances referring to tin), this is not the case for **PB2**. For the DZVP basis set the Sn–N–Si'–O–Si'' skeleton is almost coplanar, with the tin and oxygen atoms in cis positions, as can be seen by inspection of the torsional angles (see Table 2). In the case of the 6-31G(d)+PP basis the Sn and Si'' groups are located on the same side with respect to the N–Si'–O triangle. In all other cases (**PA**

(26) Frainnet, E.; Duboudin, F.; Dabescat, F.; Vincon, G. *C. R. Acad. Sci., Ser. C* **1973**, *276*, 1469.

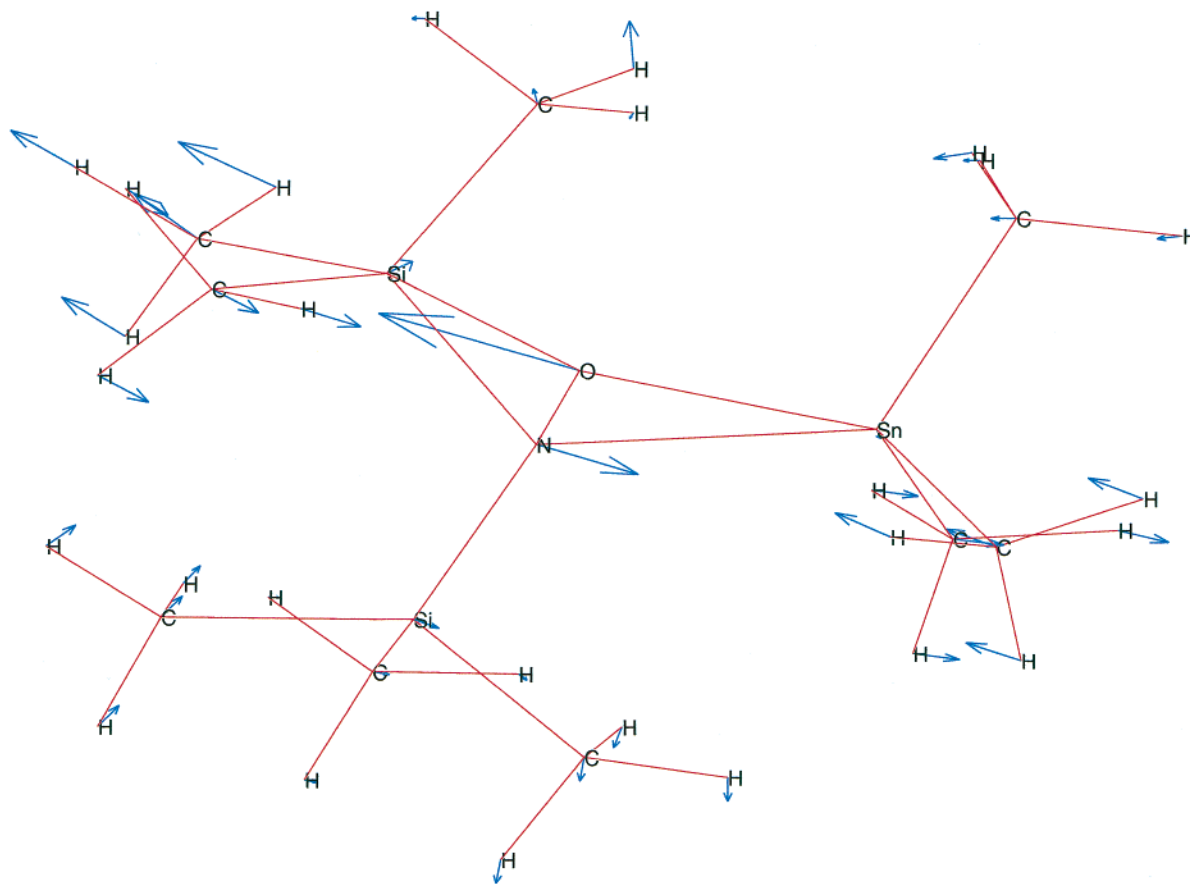


**Figure 4.** Reaction coordinate  $Q_{\text{TSD}}$  (i.e. the normal coordinate of the mode with the imaginary vibrational frequency  $\omega_{\text{TSD}}$ ) at the saddle point **TSd** corresponding to the dyotropic transition state.

and **PB1**), the terminal groups are located at opposite sides with respect to the central triatomic unit.

The Sn–O bond distances are reduced by 2.2 (**PA**) and 2.3 pm (**PB1**) when going from the DZVP to the 6-31G(d)+PP basis set, whereas the Sn–N distances are decreased by 1.7 (**PB1**) and 1.4 pm (**PB2**). The other geometrical parameters are very similar to the data reported for the various disiloxanes.<sup>8</sup> An exception is the N–O distance in **PB1** (with central Sn atom), which is increased to 332.1 pm (DZVP) and 328.4 pm (6-31G(d)+PP), respectively.

The geometries of the saddle points leading to the products discussed above are given in Table 2. The geometrical parameters are overall very similar to the respective values for the saddle points for silyl insertions in tris(silyl)hydroxylamines.<sup>8</sup> The N–O distance in **TSB1** (inserting stannyl group; see Figure 5) is ca. 24 pm larger than in the other two saddle point structures. In **TSB2**, the Si'–N–Sn angle changes from 131° (B3LYP/DZVP) to 89° (B3LYP/6-31G(d)+PP).

**PB2** is the most stable product, according to calculations with all the methods and basis sets reported in Table 3. This may be explained by the two relatively strong Si–O bonds. Product **PB1** with the inserted stannyl group is less probably formed under thermodynamic control. The most probable product is **PB2**, which is obtained through insertion of a silyl group into the N–O bond starting from isomer **B**.

Under kinetic control the insertion of a silyl group, yielding product **PB2**, is favored because the classical barrier is lower than for the other two reaction path-

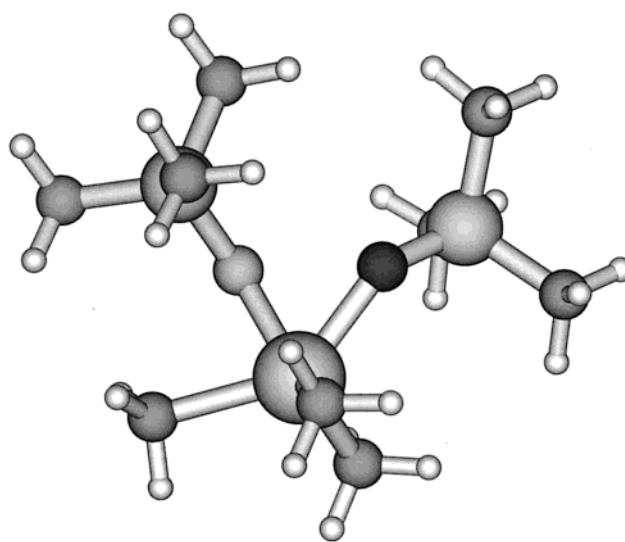


**Figure 5.** B3LYP/6-31G(d)+PP structure of the transition state for insertion of the stannyl group into the hydroxylamine N–O bond (**TSA**). See the text and Figure 2 for details.

ways. The saddle point for insertion of a stannyl group is highest in energy, so that this reaction pathway is at a disadvantage from both the thermodynamic and the kinetic points of view. Kinetically, this is certainly due to the unfavorable steric situation with the large tin atom. Thermodynamically, Si–N and Si–O bonds are stronger than Sn–N and Sn–O bonds, respectively, so



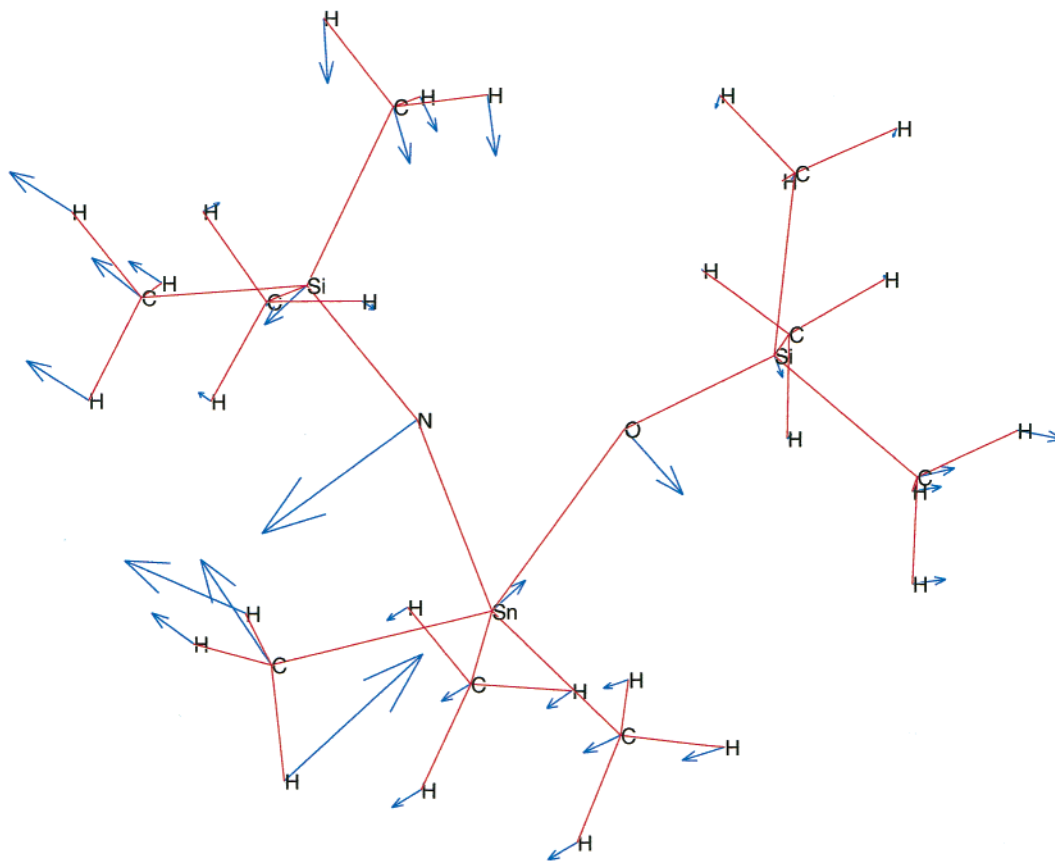


**Figure 6.** Reaction coordinate  $Q_{\text{TSA}}$  (i.e. the normal coordinate of the mode with the imaginary vibrational frequency  $\omega_{\text{TSA}}$ ) at the saddle point **TSA** for insertion of a stannyl group into the N–O bond.

that an inserted silyl group yields a lower internal product energy than an inserted stannyl group.

MP2/6-31G(d)+PP calculations yield much higher energies for the energetics of the saddle points. The increase by 14 kcal mol<sup>-1</sup> for **TSA** and **TSB2** is comparable with, but slightly smaller than the situation in ref 8. The saddle point for stannyl group insertion, however, is higher by 21 kcal mol<sup>-1</sup> compared to the B3LYP data. This large increase is mainly due to the fact that MP2 is not capable of describing such a ‘loose’ transition state correctly. The method works much better for ‘tight’ transition states such as **TSd** (see Sec. 3.2).

The harmonic vibrational frequencies of the reactive normal modes at the transition states are comparable with the data for silyl group migration<sup>8</sup> (510 and 532 cm<sup>-1</sup> for **TSA** and **TSB2**, respectively). The harmonic vibrational frequency for stannyl insertion is calculated to be 311 cm<sup>-1</sup>, indicating that the stannyl group motion is crucial during the passage of the transition state. In Figure 6, the motion is graphically displayed: the nitrogen and the oxygen atoms move apart, and the tin atom inserts. Simultaneously, the nitrogen atom and one of the carbon atoms of the stannyl group approach each other and a new N–C bond is formed. The harmonic vibrational frequencies of the reactive normal modes of the transition states discussed in this work as well as the pertinent reduced masses are collected in Table 4.

In summary, a stannyl group insertion will not be possible. It is inhibited for both kinetic and thermodynamic reasons. A silyl group insertion is more likely to

**Table 4.** Harmonic Vibrational Frequencies  $\omega_{\text{TS}}$  (in cm<sup>-1</sup>) of the Reactive Normal Coordinates  $Q_{\text{TS}}$  of the Transition States (**TSd**, **TSA**, **TSB1**, and **TSB2**)<sup>a</sup>

	<b>TSd</b>	<b>TSA</b>	<b>TSB1</b>	<b>TSB2</b>
$\omega_{\text{TS}}$	230.85	509.86	311.38	531.61
$\mu_{\text{TS}}$	9.34	9.21	8.50	9.23

<sup>a</sup> The corresponding reduced masses (in amu) are denoted by  $\mu_{\text{TS}}$  (B3LYP/6-31G(d)+PP results).

occur. It should be noted that stannyl group insertion may be possible in tris(stannyl)hydroxylamines. It would be most desirable to synthesize such species and to find experimental conditions where a stannyl insertion becomes possible.

#### 4. Conclusions

With *O*-lithium-*N,N*-bis(*tert*-butyldimethylsilyl)hydroxylamide as the starting material, *N,O*-bis(*tert*-butyldimethylsilyl)-*N*-(trimethylstannyl)hydroxylamine was prepared. This implies an N–O silyl group and an O–N stannyl group migration.

To understand the mechanisms of the rearrangement reactions in the bis(silyl)stannylhydroxylamine system, quantum-chemical calculations with the permethylated *N,N*-bis(silyl)-*O*-stannylhydroxylamine were carried out. Density functional calculations, with and without employment of a pseudopotential, reveal the existence of a dyotropic transition state with a classical barrier height of 28 kcal mol<sup>-1</sup> (B3LYP). The angle at the migrating stannyl group measures only 39.5°. The



isomeric *N,O*-bis(silyl)-*N*-stannylhydroxylamine produced in this isomerization is only 2 kcal mol<sup>-1</sup> more stable than the primarily formed *N,N*-bis(silyl)-*O*-stannylhydroxylamine. Furthermore, the possibility of a stannyl group insertion into the N–O bond was studied which may take place in analogy to the silyl group insertion.<sup>8</sup> It was found that silyl group insertion is more favorable than stannyl group insertion, for both kinetic and thermodynamic reasons. However, in principle stannyl group insertion appears to be possible: e.g. in tris(stannyl)hydroxylamines. Work in this direction is in progress in our laboratories.

## 5. Experimental Section

All experiments were performed in oven-dried glassware under purified nitrogen or argon using standard inert-atmosphere and vacuum-line techniques. All NMR spectra were obtained on a Bruker AM-250, MSL-400, or Avance 500 spectrometer with SiMe<sub>4</sub> as internal reference or SnMe<sub>4</sub> as external reference. The mass data are reported in mass to charge units (*m/z*) with their relative intensities in parentheses. The NMR spectra confirmed the purity of **1**.

***N,O*-Bis(*tert*-butyldimethylsilyl)-*N*-(trimethylstannyl)-hydroxylamine (**1**)**. To a solution of 13.0 g (0.05 mol) of *N,O*-bis(*tert*-butyldimethylsilyl)hydroxylamine in hexane was added dropwise 21.2 mL of a solution of *n*-butyllithium in hexane (23%). The mixture was heated to reflux for 3 h. The white suspension was added dropwise to 10.0 g (0.05 mol) of Me<sub>3</sub>SnCl in THF at –35 °C. The mixture was warmed to ambient temperature and refluxed for 3 days. After the mixture was cooled to room temperature, the product was separated from LiCl by centrifuging. The clear liquid obtained was fractionally distilled under reduced pressure to yield 9.6 g (45%) of **1**. Bp: 84 °C/0.05 Torr. <sup>1</sup>H NMR (CDCl<sub>3</sub>): δ 0.94

(s, 9H, NSiC(CH<sub>3</sub>)<sub>3</sub>), 0.89 (s, 9H, OSiC(CH<sub>3</sub>)<sub>3</sub>), 0.33 (s, 9H, Sn(CH<sub>3</sub>)<sub>3</sub>), 0.09 (s, 6H, NSi(CH<sub>3</sub>)<sub>2</sub>), 0.02 (s, 6H, OSi(CH<sub>3</sub>)<sub>2</sub>). <sup>13</sup>C NMR (CDCl<sub>3</sub>): δ 28.12 (s, NSiC(CH<sub>3</sub>)<sub>3</sub>), 26.56 (s, OSiC(CH<sub>3</sub>)<sub>3</sub>), 19.84 (s, NSiC(CH<sub>3</sub>)<sub>3</sub>), 18.71 (s, OSiC(CH<sub>3</sub>)<sub>3</sub>), –2.53 (s, NSi(CH<sub>3</sub>)<sub>2</sub>), –3.10 (s, Sn(CH<sub>3</sub>)<sub>3</sub>), –3.76 (s, OSi(CH<sub>3</sub>)<sub>2</sub>). <sup>29</sup>Si NMR (CDCl<sub>3</sub>): δ 22.80 (s, OSi), 12.80 (s, NSi). <sup>119</sup>Sn NMR (CDCl<sub>3</sub>): δ 71.85 (s, Sn). MS (EI): *m/z* 424 (1) [M<sup>+</sup>].

**Crystal Structure Solution and Refinement for **1** (Table 1)**. Data for structure **1** were collected on a Stoe IPDS II diffractometer with a Siemens image plate by use of  $\varphi$  and  $\omega$  scans. A semiempirical absorption correction was applied. The structure was solved by direct methods (SHELXTL<sup>27</sup>) and refined against  $F^2$  using SHELXL-97. All non-hydrogen atoms were refined anisotropically. For the hydrogen atoms a riding model was employed.

**Acknowledgment.** S.S. is indebted to Prof. P. Botschwina for his continuous support. Fruitful discussions with Dr. F. Diedrich, Dr. R. Oswald, and Prof. D. R. Salahub are gratefully acknowledged. Dr. Oswald is also acknowledged for his help in preparing Figures 4 and 6. Some of the calculations were carried out at the Gesellschaft für wissenschaftliche Datenverarbeitung Göttingen (GWDG). Support of this work by the Deutsche Forschungsgemeinschaft and the Fonds der Chemischen Industrie is gratefully acknowledged.

**Supporting Information Available:** Table of crystal data, complete fractional coordinates, bond lengths and angles, and anisotropic displacement parameters of the structure of **1**. This material is available free of charge via the Internet at <http://pubs.acs.org>.

OM0206195

(27) Sheldrick, G. M. Program SHELXL-97; Universität Göttingen, Göttingen, Germany, 1997.